Temporal patterns of phytoplankton assemblages, size spectra and diversity during the wane of a *Phaeocystis globosa* spring bloom in hydrologically contrasted coastal waters

MATHILDE SCHAPIRA[1], DOROTHEE VINCENT[2], VALERIE GENTILHOMME[3] AND LAURENT SEURONT[1,3,4]

[1]School of Biological Sciences, Flinders University, GPO Box 2100, Adelaide SA 5001, Australia, [2]Laboratoire Ecosystèmes Littoraux et Côtiers, Maison de la Recherche en Environnement Naturel, CNRS FRE 2816 ELICO, Université du Littoral-Côte d'Opale, 32 Avenue Foch, 62930 Wimereux, France, [3]Laboratoire Ecosystèmes Littoraux et Côtiers, Station Marine de Wimereux, CNRS FRE 2816 ELICO, Université des Sciences et Technologies de Lille 1, 28 Avenue Foch BP-80, 62930 Wimereux, France, [4]South Australian Research and Development Institute, Aquatic Sciences, West Beach, SA 5022, Australia

The space–time dynamic of phytoplankton diversity and succession was investigated during the wane of a Phaeocystis globosa *spring bloom in four distinct hydrological sub-systems of the eastern English Channel. Nutrients, chlorophyll-a concentrations, and phytoplankton composition, standing stocks, size spectra and diversity were monitored during three key periods in 2003: late spring, early summer and summer. Two consecutive diatom assemblages were observed, respectively dominated by: (i) small colonial species (<100 μm;* Melosira *sp.,* Diploneis *sp. and* Navicula transitans*) in April; and (ii) large fine-walled cells (>200 μm;* Guinardia striata *and* Rhizosolenia imbricata*) in May and July. This shift in diatom composition appeared to be related to the potentially limiting silicic acid in early summer. Specific phytoplankton assemblages identified in distinct water masses have evolved from a mature/senescent community towards a relatively homogeneous aestival structure of dominant species that might have been triggered by the wane of the* P. globosa *bloom. Our results also identified a strong heterogeneity in the distribution of secondary species between distinct water masses during the summer period, suggesting that the magnitude of the observed patterns was intrinsically related to the hydrological properties prevailing in each sub-system. The identification of distinct temporal patterns in phytoplankton species diversity and succession following the wane of a spring bloom at relatively small spatial scales (i.e. <10 km) is discussed in the framework of* P. globosa *blooms in particular and phytoplankton blooms in general and is suggested to have potentially strong consequences on food web dynamics and the carbon cycle in coastal ecosystems.*

INTRODUCTION

The space–time dynamics of phytoplankton populations has been widely investigated with a special focus on the impact of hydrological conditions on spatial distribution and succession patterns (e.g. Chang *et al.*, 2003; Badylak & Phlips, 2004; Estrada *et al.*, 2004, and references therein). Large diatoms (>30 μm) typically dominate phytoplankton spring blooms due to their high ability to use winter nutrient stocks and increasing irradiance (Harris, 1978; Chang, 1980). The late spring collapse of the diatom bloom coincides with decreasing nutrient levels and is followed by a drastic shift in phytoplankton composition towards pico- and nanophytoplankton

(Sin *et al.*, 2000; Tadonléké & Sime-Ngando, 2000) and motile microphytoplankton cells (i.e. flagellates and dinoflagellates; Chang *et al.*, 2003; Bode *et al.*, 2005) which prevail during the summer. This generally fuels the microbial loop and short-circuits the classical herbivorous food chain (Azam *et al.*, 1983), thus profoundly affecting the food-web structure. However, the qualitative and quantitative nature and the potential consequences of this shift have barely been investigated in most marine ecosystems. In particular, we are not aware of any study investigating the dynamics of species diversity and succession in relation to the wane of a nearly monospecific bloom occurring in hydrologically contrasted coastal waters.

In the coastal waters of the eastern English Channel, the phytoplankton spring bloom is characterized by the recurrent proliferation of *Phaeocystis globosa* (e.g. Seuront *et al.*, 2006). This algal species is known to form massive blooms in many environments, often resulting in a distortion of the pelagic

Corresponding author:
M. Schapira
Email: mathilde.schapira@flinders.edu.au

ecosystem (Hamm, 2000). In the eastern English Channel, *P. globosa* blooms typically follow and precede two distinct diatom assemblages and abruptly collapse at the end of spring (Breton *et al.*, 2000; Seuront *et al.*, 2006). In the Southern Bight of the North Sea, where the phytoplankton spring bloom is also dominated by *P. globosa* (Lancelot *et al.*, 1994; Rousseau *et al.*, 1994; Lancelot, 1998), similar spring phytoplankton community successions have been observed (Gieskes & Kraay, 1975; Cadée & Hegeman, 1986; Rousseau *et al.*, 2002; Stelfox-Widdicombe *et al.*, 2004). Phytoplankton seasonal production and its relation to nutrient cycles have previously been investigated in the eastern English Channel (Brunet *et al.*, 1992, 1996; Gentilhomme & Lizon, 1998; Breton *et al.*, 2000; Seuront *et al.*, 2006). However, to our knowledge, the size-structure and diversity of phytoplankton assemblages still need to be documented, especially in relation with the decline of the *P. globosa* spring bloom.

The objective of the present study was to provide further insights into the consequence of the *P. globosa* spring bloom on the dynamics of phytoplankton succession in the eastern English Channel. In particular, this area is characterized by strong hydrological inshore/offshore and north/south gradients respectively linked to: (i) the residual circulation of nearshore water masses parallel to the coast drifting from the English Channel to the North Sea; and (ii) to the significant decrease in riverine inputs from the Bay of Somme to the Strait of Dover. Under the hypothesis that different *P. globosa* bloom magnitude will be associated with distinct hydrological sub-systems, we investigated the temporal dynamics of phytoplankton composition, diversity and size-structure during the late phase (April–July) of a *P. globosa* bloom in the inshore and offshore waters of the Bay of Somme and the Strait of Dover.

MATERIALS AND METHODS

Study area

The eastern English Channel is characterized by a large tidal range, between 3 to 9 m. The tidal regime generates a residual circulation parallel to the coast, referred to as the 'coastal flow' (Brylinski *et al.*, 1991) with nearshore coastal waters drifting from the English Channel into the North Sea. This coastal flow generates a tidally controlled frontal zone (Brylinski & Lagadeuc, 1990; Lagadeuc *et al.*, 1997) that separates inshore and offshore water masses. Inshore water masses are characterized by their low salinity, high turbidity, high phytoplankton richness (Brylinski *et al.*, 1984) and high productivity (Brunet *et al.*, 1992, 1993) compared to the oceanic offshore waters. The eastern English Channel is also hydrologically structured along a north/south gradient, in relation to the differential riverine inputs from the Bay of Somme to the Strait of Dover (Figure 1). The south of the eastern English Channel and the Bay of Somme are protected from the northerly winds and strongly influenced by high freshwater discharge from the Somme River (mean annual flow: 35 $m^3\ s^{-1}$; Brylinski *et al.*, 1984) and its related nutrient enrichment. In contrast, the Strait of Dover is characterized by higher hydrodynamic conditions than the Bay of Somme related to its shallow waters and strong tidal currents (Seuront, 2005) and comparatively weakly influenced by the
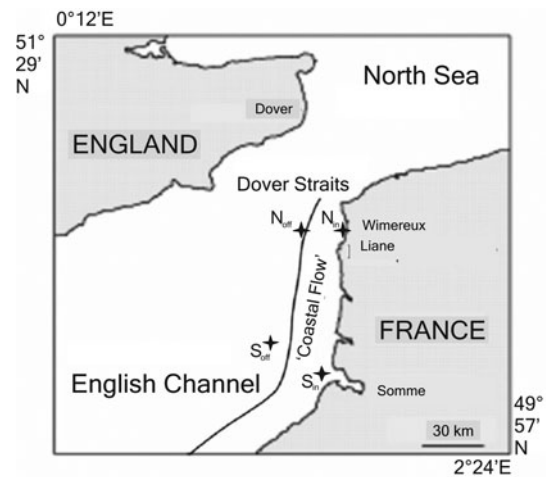

Fig. 1. Study area and location of the sampling stations (+), S_{in} (50°48′N–1°34′E), S_{off} (50°48′N–1°27′8″E), N_{in} (50°14′39″N–1°26′47″E) and N_{off} (50°20′33″N–1°1′053″E).

small run-off of the Liane and Wimereux rivers (mean annual flow: 0.6 and 0.1 $m^3\ s^{-1}$, respectively; national data bank for hydrometry and hydrology of the French Ministry of the Environment; http://hydro.rnde.tm.fr/accueil.html).

Sampling strategy

Three cruises were conducted in 2003 during late spring (22–23 April), early summer (13–15 May) and summer (6–10 July) aboard NO 'Côtes de la Manche' (CNRS, INSU). Two sampling areas, located in the northern and southern part of the eastern English Channel, were specifically chosen because of the significant differences in their physical and hydrological properties, especially their nutritive status which is likely to affect phytoplankton growth and hence phytoplankton stocks and composition. Inshore and offshore waters of each site were sampled over the same day and both sites were studied within 1 to 4 days (Table 1). No sampling was conducted in the southern offshore station in May (Table 1). Hereafter sampling stations are referred to as N_i and S_i, where 'N' and 'S' are the north and south of the eastern English Channel, and the subscript 'in' and 'off' represent the sampling location, inshore and offshore respectively.

For each sampling date wind speed (m s^{-1}) and direction were obtained from the Météo France Centre of Boulogne-sur-Mer. Temperature and salinity profiles were collected at each sampling station with a SBE 25 Sealogger CTD. Water samples for hydrological (nutrients) and biological parameters (chlorophyll-*a*, protists' biomass, standing stocks and composition) were taken from sub-surface (1 m) using 5-l Niskin bottles. Only sub-surface samples were considered because previous surveys conducted in the eastern English Channel showed the water column to be vertically well mixed (e.g. Gentilhomme & Lizon, 1998; Seuront *et al.*, 2006) in accordance with recent estimates of turbulent energy dissipation rates ranging from 10^{-7} to 10^{-4} $m^2\ s^{-3}$ (Seuront, 2005). In addition, sub-surface sampling allowed to avoid any contamination of our samples by benthic and tychoplanktonic phytoplankton. The latter are resuspended in the bottom layer of the water column (Dupont *et al.*,

Table 1. *In situ* conditions at the sampling periods: locations, dates, depths, tidal and wind conditions.

Period	Stations	Dates	Depth (m)	Tide	F/E	Wind speed (m s^{-1})	Wind direction
April	N_{in}	22 April	16.9	NT	F	4.0	NE
	N_{off}	22 April	56.5	NT	E	4.0	NE
	S_{in}	23 April	13.4	NT	E	6.0	NE
	S_{off}	23 April	36.4	NT	F	6.0	NE
May	N_{in}	15 May	20.7	ST	F	3.0	S–SE
	N_{off}	15 May	54.1	ST	F	3.0	S–SE
	S_{in}	13 May	18.9	MT	F	7.0	W
	S_{off}	–	–	–	–	–	–
July	N_{in}	6 July	X	NT	E	4.0	S–SW
	N_{off}	6 July	X	NT	F	4.0	S–SW
	S_{in}	10 July	12.9	NT	E	3.0	S
	S_{off}	10 July	20.7	NT	E	3.0	S

MT, mid-tide; ST, spring tide; NT, neap-tide; F, flood tide; E, ebb tide. (–) no sampling could be conducted due to weather conditions. X, data not available.

1991; Huaut *et al.*, 1994) and their proportion being highly variable at different time scales (Wolfstein *et al.*, 2000) and strongly depending on the energy dissipation rates of the environment (e.g. spring–neap cycle, season, wind stress; Grabemann & Krause, 2001).

Nutrient analysis

For dissolved inorganic nutrients (NO_2^- NO_3^-, $Si(OH)_4$, HPO_4^{2-}) 10-ml water samples were immediately frozen ($-20°C$) after field collection, and analysed in the laboratory with an auto-analyser (Alliance Integral Futura) following standard protocols (Bendschneider & Robinson, 1952; Mullin & Riley, 1955; Murphy & Riley, 1962; Woods *et al.*, 1967). Ammonium (NH_4^+) concentrations were determined manually in 100-ml water samples following Koroleff (Koroleff, 1969).

The potential limitation of phytoplankton growth by nutrient availability was investigated through the comparison between N:P:Si ratios of water masses and standard Redfield ratio (Redfield *et al.*, 1963; Brzezinski, 1985). Data points obtained during the survey were plotted in a synthetic graph of Si:N:P molar ratios, where the conditions Si:N $= 1$, N:P $= 16$ and Si:P $= 16$ define 6 areas, each of them being characterized by the potentially limiting nutrient in order of priority.

Phytoplankton analysis

Water samples (200 to 1000-ml) were filtered through glass-fibre filters (Wahtman GF/C) and immediately frozen ($-20°C$) until analysis. Chlorophyll pigments were subsequently extracted in 5-ml of 90% acetone in the dark at $4°C$ during 24 hours, assayed in a spectrophotometer (UVIKON 940, Kontron instruments®) and Chl *a* concentrations calculated following UNESCO standard calculation (UNESCO, 1966).

The study of auto- and hetero/mixotrophic protists was carried out on organisms ranging in size from 5 to >200 μm. 100-ml water samples were fixed with acid Lugol solution (2% final concentration) and stored in the dark at 4 °C. In the laboratory, 10 to 20-ml sub-samples were settled for >24 h in Hydro-Bios counting chambers (Utermöhl, 1958). An average of 860 ± 250 cells was counted (Venrick, 1978). Phytoplankton identification was performed by inverted microscopy under contrast illumination (e.g. Hasle *et al.*, 1997; Paulmier, 1997) using a Leitz Diavert microscope ($\times 200$, $\times 400$ and $\times 630$). Cells were measured with an eyepiece micrometer and corresponding biovolumes were calculated by relating the shape of organisms to a standard geometric form (Hillebrand *et al.*, 1999; Sun & Liu, 2003). Biovolumes were converted to carbon biomass following Menden-Deuer & Lessard (2000) & Menden-Deuer *et al.* (2001). *Phaeocystis globosa* biomass was estimated from total cell counts (Van Rijssel *et al.*, 1997). The year 2003 was characterized by an early and short-term *P. globosa* bloom which peaked in early March 2003 (Lamy *et al.*, 2006; Muylaert *et al.*, 2006) and disappeared rapidly by the end of April. Thus no or few colonies were observed in our samples. We therefore assumed that their contribution to carbon biomass was negligible. In addition, as *P. globosa* flagellate cells outnumbered other flagellate species throughout the survey (e.g. *Chrysomonas* and *Cryptomonas*) the latter were pooled in a common group hereafter referred to as *PgF*. The settlement method presented above (10 to 20-ml sub-samples) is not reliable for the quantitative study of ciliated protozoans. However, the observation of these organisms, namely *Acineta* sp., Tintinnids and Aloricate ciliates, allowed us to estimate their relative contribution to the protist pool. Some of the dinoflagellates counted during the survey (*Gyrodinium* sp. and *Gyrodinium lachryma*) appeared to be heterotrophic and cannot be thought of as phytoplankters *sensu stricto*. Subsequently and for the sake of simplicity they will be hereafter analysed separately from true phytoplankters.

Phytoplankton size-structure was studied through five major size-categories within which the smallest and largest forms were respectively dominated by *Cryptophyta* sp. and *P. globosa* (5 μm in length), and the diatoms *Rhizosolenia setigera* and *Rhizosolenia imbricata* (300–400 μm in length). Two different size-categories were set for nanophytoplankton (≤ 10 μm, 10–20 μm) and 3 for microphytoplankton (20–100 μm, 100–200 μm, >200 μm).

Data analysis

As the distribution of temperature and salinity data were significantly not normal, non-parametric statistics were used in this study. For each sampling period, multiple comparisons between the four sampling stations were conducted using the

Kruskal–Wallis test (KW test hereafter). When the KW test identified a significant difference ($P < 0.05$), a post-hoc comparison, conceptually similar to the Tukey's HSD procedure (Zar, 1996) was performed to identify significant differences.

Multivariate analysis was carried out to identify phytoplankton species assemblages and to describe their spatial and temporal variability. A factor analysis (Legendre & Legendre, 1998) was applied to the whole data set of phytoplankton (38 taxa matrix) to assess the global distribution of phytoplankton communities within the four sub-systems.

Species richness (i.e. the number of different species in a given station at a given date, S), diversity (H') and evenness (J') were calculated on autotrophic protists following Shannon & Weaver (1963) and Pielou (1966):

$$H' = -\sum_{i=1}^{S} f_i \log_2 f_i \qquad (1)$$

$$J' = \frac{H'}{\log_2 S} \qquad (2)$$

where f_i is the relative frequency of species i in the sample. Potential changes in the structure of phytoplankton communities were further investigated through rank–frequency diagrams (RFDs; Frontier, 1976). This technique relies on plotting species frequencies against their ranks organized in decreasing order, and with both axes in logarithmic scale (Frontier, 1985; Legendre & Legendre, 1998). Changes in the shape of the RFDs characterize temporal changes in the community structure (Frontier, 1985). More specifically, a linear–concave curve (or S-shaped curve) indicates the dominance of 1 or 2 species in a low species richness assemblage (stage 1, pioneer community). In contrast, a more convex shape among the first ranked species indicates a more even distribution among dominant species (stage 2, mature community), and a linear RFD is observed at the end of an ecological succession when the first ranked species become more dominant and the species richness is also lower (stage 3, senescent community). After a disturbance, few species can quickly develop (i.e. 'r strategists' and 'opportunists') and the RFD appears coarsely rectilinear with successive steps (stage 1', intermediate stage between stages 1 and 2; Frontier, 1985; Legendre & Legendre, 1998). In addition, the occurrence of assemblages exhibiting the same diversity, evenness and RFD shape, was investigated by calculating the average distance between rank distributions. A distance is here defined as a quantitative measure of the difference in rank distribution of given species between 2 distinct samples. For a given phytoplankton species, (P_1), the distance (d) between its rank in samples 1 and 2 can thus be given by (Seymour *et al.*, 2004):

$$d_{12}(P_1) = [r_1(P_1) - r_2(P_1)]^{1/2} \qquad (3)$$

where, $r_1 (P_1)$ is the rank of species P_1 in sample 1 and $r_2 (P_1)$ is the rank of the same species in sample 2. The total distance between the two samples, incorporating all phytoplankton species, (P_i), is defined as the mean square root distance between the ranks of all common species (Seymour *et al.*, 2004):

$$d_{12} = \left[\frac{1}{N} \sum_{i=1}^{N} (r_1(P_i) - r_2(P_i))^2 \right]^{1/2} = \left[\frac{1}{N} \sum_{i=1}^{N} r_{12}^2(P) \right]^{1/2} \qquad (4)$$

where N is the total number of common species, (P_i), observed in both samples. This quantification of distances between rank distributions was employed as an indication of differences in community structure between the four sampling sites over the survey period.

RESULTS

Physical environment

The study period was characterized by excess insulation (30% higher than the monthly mean insulation calculated over a decade) and punctual storm events in May and July (11–24 May; 16 July). The wind regime is congruent with Pingree & Griffiths (1980) and Salomon & Breton (1991), and was characterized by the dominance of south-westerly winds during much of the study period (May to July). April was characterized by north-eastern winds enhancing the continental influence on water masses. Wind speed did not show any specific pattern with values ranging from 3 to 7 m s^{-1} during May storm events (Table 1). After a sharp decrease from 58.2 to 45.4 m^3 s^{-1} on 21 April, River Somme inputs followed a decreasing trend throughout the study period (from 60.5 to 27.3 m^3 s^{-1}) characterized by small fluctuations (± 6 m^3 s^{-1}; Figure 2).

No vertical stratification was observed over the course of the survey. Vertically averaged salinity did not exhibit any temporal pattern, and slightly fluctuated between 33.27 $\pm$ 0.17 (S_{in}-April) and 34.89 $\pm$ 0.02 (S_{off}-April; Table 2). In contrast, vertically averaged temperature exhibited a clear seasonal cycle, increasing gradually from 8.9 $\pm$ 0.1°C (N_{off}-April) to 18.7 $\pm$ 0.2°C (S_{in}-July; Table 2). These temperature and salinity values were consistent with previous measurements performed at the seasonal scale in this area (Brunet *et al.*, 1992; Brylinski *et al.*, 1996; Breton *et al.*, 2000; Schapira, 2005; Seuront *et al.*, 2006).

The four sampling stations exhibited significantly different temperatures and salinities (KW test; $P < 0.05$) over the study period. The highest temperatures ($P < 0.001$) and lowest salinities ($P < 0.001$) were recorded in S_{in} throughout the survey. Although the influence of riverine inputs is less important in the Strait of Dover, coastal water masses (N_1) were consistently significantly different (higher temperature and lower salinity; $P < 0.001$) from the offshore ones. No significant differences were observed between N_{off} and S_{off} in terms of temperature and salinity.
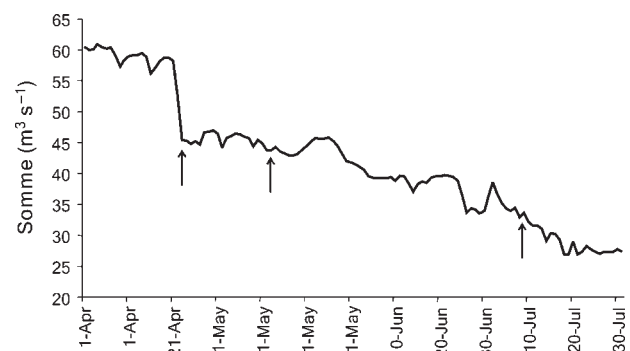

Fig. 2. Daily Somme river inputs (m^3 s^{-1}) recorded on the study site from April to July 2003. Black arrows correspond to sampling periods.

Table 2. Vertically averaged ($\pm$ SE) salinity (S) and temperature (T). Nitrite + nitrate ($NO_2^- + NO_3^-$), ammonium (NH_4^+), silicic acid ($Si(OH)_4$), phosphate (HPO_4^{2-}) concentrations (μM) and chlorophyll-a ([Chl a]) surface concentrations ($\mu g\,l^{-1}$) recorded on the sampling stations N_{in}, N_{off}, S_{in} and S_{off} during the survey. No data were available for S_{off} in May. DL, detection limit.

Station	Period	S (PSU)	T (°C)	$NO_2^- + NO_3^-$ (μM)	NH_4^+ (μM)	$Si(OH)_4$ (μM)	HPO_4^{2-} (μM)	[Chl a] ($\mu g\,l^{-1}$)
N_{in}	April	33.88 ± 0.03	9.6 ± 0.0	0.31	0.0	0.65	0.40	1.3
	May	34.31 ± 0.05	11.8 ± 0.1	<DL	0.4	<DL	0.71	1.8
	July	34.22 ± 0.00	16.5 ± 0.0	<DL	1.0	0.94	0.19	5.9
N_{off}	April	34.65 ± 0.03	8.9 ± 0.1	0.16	0.0	0.17	0.13	0.8
	May	34.87 ± 0.02	11.1 ± 0.0	<DL	0.6	<DL	0.19	3.4
	July	34.52 ± 0.10	15.5 ± 0.3	0.07	0.6	2.44	0.50	2.2
S_{in}	April	33.27 ± 0.17	10.1 ± 0.1	0.54	0.2	1.24	0.65	7.9
	May	33.91 ± 0.00	12.5 ± 0.0	0.11	0.3	<DL	0.69	4.4
	July	33.30 ± 0.16	18.7 ± 0.2	0.08	0.4	0.93	0.13	5.7
S_{off}	April	34.89 ± 0.02	9.1 ± 0.1	0.27	0.0	0.86	0.41	0.9
	May	–	–	–	–	–	–	–
	July	34.65 ± 0.06	16.2 ± 0.1	<DL	0.3	0.69	0.11	2.0

Chemical environment

The highest $NO_2^- + NO_3^-$ concentrations were recorded in April and ranged from 0.16 to 0.31 μM and from 0.27 to 0.54 μM in the Strait of Dover and the Bay of Somme, respectively (Table 2). Concentrations then decreased to levels close to the detection limit, i.e. <0.05 μM, in July. Ammonium concentrations were always lower than 1 μM, but increased gradually from April to July (Table 2). $Si(OH)_4$ concentrations always remained lower than 2.5 μM and decreased below the detection limit from April to May in all locations. They subsequently increased in July and ranged between 0.94 and 2.44 μM in the Strait of Dover and between 0.69 and 0.93 μM in the Bay of Somme. HPO_4^{2-} concentrations remained lower than 0.8 μM and did not exhibit any specific pattern throughout the sampling period. The lowest concentrations were recorded in July in the Bay of Somme with 0.13 and 0.11 μM in inshore (S_{in}) and offshore (S_{off}) waters, respectively. The highest concentrations were observed in coastal waters S_{in} (0.69 μM) and N_{in} (0.71 μM) in May.

Molar ratios for silicic acid, DIN ($NO_2^- + NO_3^- + NH_4^+$) and phosphate (Figure 3) showed distinct patterns of potential nutrient limitation during each sampling cruise. In April, DIN was the potentially limiting nutrient in the whole area, followed by silicate (Si:P ratios: 1.3–2.1). In May, the decrease

in Si:N ratios (values close to 0) and the low N:P ratios (0.6–3.0) illustrated a potential limitation of primary production by $Si(OH)_4$ and DIN. As observed in April, both DIN and silicate were potentially limiting summer phytoplankton growth although higher N:P and Si:P ratios observed at that time indicated a potentially weaker summer limitation.

Phytoplankton standing stocks

Chl a concentrations were highly variable between sites in April and May, ranging from 0.8 $\mu g\,l^{-1}$ in N_{off} to 7.9 $\mu g\,l^{-1}$ in S_{in} in April, and from 1.8 $\mu g\,l^{-1}$ in N_{in} to 4.4 $\mu g\,l^{-1}$ in S_{in} in May (Table 2). However, in July, inshore water masses exhibited similar concentrations reaching 5.9 $\mu g\,l^{-1}$ in N_{in} and 5.7 $\mu g\,l^{-1}$ in S_{in}. In offshore waters a 2-fold decrease in Chl a concentrations was observed with 2.0 $\mu g\,l^{-1}$ in S_{off} and 2.2 $\mu g\,l^{-1}$ in N_{off}.

Thirty-eight taxa were identified throughout the survey and distributed in four taxonomic classes: diatoms (28), dinoflagellates (8), cryptophyceans (1) and prymnesiophyceans (1). Total phytoplankton abundance and biomass ranged from 69.1×10^3 to 441.8×10^3 cell l^{-1} and from 49.4 to 1181.3 $\mu gC\,l^{-1}$, respectively (Table 3). However, no common temporal pattern could be identified for the four sampling stations. Diatoms constituted the bulk of phytoplankton assemblages (34–97% of total abundance) with abundance ranging between 36.1×10^3 and 410.3×10^3 cell l^{-1} and relative biomass accounting for 58 to 99% of total phytoplankton carbon. Although *PgF* was the second dominant group ranging between 0.0 and 169.4×10^3 cell l^{-1} (i.e. <1 to 51.1% of total abundance), these small sized cells only had a small and punctual contribution to total carbon biomass (<1–25%). Microscopic observations only revealed few colonial stages and most of *P. globosa* cells were at that time isolated flagellate cells. In addition, qualitative observation of ciliated protozoans showed an increase in total ciliates per sample in April, and coincided with the end of the *P. globosa* bloom. Despite their poor contribution to total phytoplankton carbon (≤ 0.1 $\mu gC\,l^{-1}$), cryptophyceans were numerically the third dominant group with abundance values of 0.0 to 42.8×10^3 cell l^{-1} (i.e. <1 to 31% of total abundance). Dinoflagellates were far the least abundant with values ranging between 0.8×10^3 and 40.4×10^3 cell l^{-1}, representing only 1 to 11% of total phytoplankton abundance
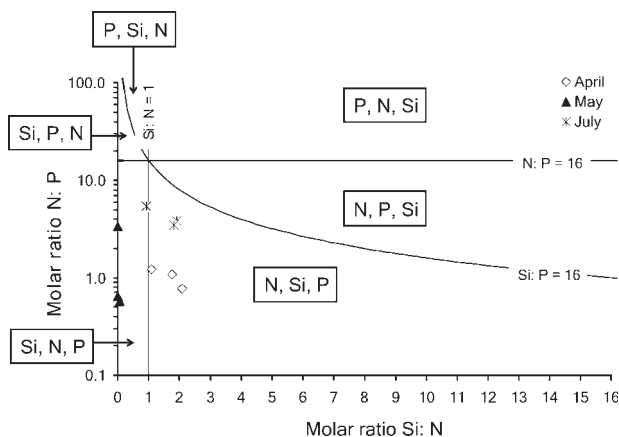
Fig. 3. Si:N:P molar ratios in April ($\diamond$), May ($\blacktriangle$) and July ($\ast$). In each area delimited by the Brzezinski (1985) ratio and the Redfield *et al.* (1963) ratio (Si:N:P = 16:16:1), the potential limiting nutrients are reported in order of priority. No data were available for S_{off} in May.

Table 3. Abundance 'A' (10^3 cell l^{-1}) and biomass 'B' ($\mu g\,C\,l^{-1}$) of major auto- and hetero/mixotrophic protists identified from Lugol's iodine-preserved samples collected on the four sampling stations N_{in}, N_{off}, S_{in} and S_{off} during the survey. No data were available for S_{off} in May.

Station	Period	PgF		Diatoms		Crypto		Auto. Dino		Hetero. Dino		Total	
		A	B	A	B	A	B	A	B	A	B	A	B
N_{in}	April	36.8	3.6	46.7	118.5	42.8	0.1	11.2	2.5	1.2	15.9	138.7	140.5
	May	9.5	<0.1	271.8	525.3	0.0	<0.1	2.6	0.5	1.0	13.2	284.9	539.0
	July	0.0	<0.1	294.4	337.4	24.0	<0.1	31.4	7.2	9.0	119.0	358.8	463.7
N_{off}	April	12.7	2.1	156.2	125.5	2.5	<0.1	6.6	0.5	1.6	<0.1	177.9	128.1
	May	6.8	<0.1	394.3	383.6	3.3	<0.1	0.6	0.1	0.2	15.9	406.2	399.6
	July	5.5	3.7	185.7	216.2	0.0	<0.1	12.8	2.0	0.0	<0.1	204.8	221.9
S_{in}	April	169.4	2.2	152.3	208.4	1.2	<0.1	0.6	0.1	8.0	105.7	331.5	316.5
	May	8.8	0.4	307.7	239.0	0.1	<0.1	4.0	1.0	13.2	171.9	334.0	412.3
	July	3.3	<0.1	410.3	1175.4	0.4	<0.1	27.8	5.9	0.0	<0.1	441.8	1181.3
S_{off}	April	29.1	12.0	36.1	36.9	0.8	<0.1	3.0	0.5	0.0	<0.1	69.1	49.4
	May	–		–		–	<0.1	–		–	<0.1	–	
	July	1.8	<0.1	169.2	207.9	0.0	<0.1	9.9	1.2	0.0	<0.1	180.9	209.1

(Table 3). Two heterotrophic forms of dinoflagellates were observed, *Gyrodinium* sp. and *G. lachryma*. Both forms were particularly abundant in S_{in}, reaching 8.0×10^3 and 13.2×10^3 cell l^{-1} in April and May, respectively. Due to their large size, *G. lachryma* (160 μm) and other heterotrophic dinoflagellates (60 μm) accounted for 33 and 42% of total carbon biomass during these periods.

The first three axes of the factor analysis described 68.1% of the total inertia (the fourth axis only explained 9% of the total inertia) and the distribution of species (Figure 4B, D) and stations (Figure 4A, C) showed the space–time dynamic of phytoplankton assemblages over the survey. The first two axes showed the succession of two characteristic phytoplankton assemblages as well as a strong spatial heterogeneity in late spring (Figure 4A, B). The first axis was structured by the opposition between the stations sampled in April characterized by *PgF* (37% of total inertia) along with small diatoms (e.g. *Melosira* sp., *Diploneis* sp. and *N. transitans*) and the stations sampled in May and July characterized by large diatoms (*G. striata* and *R. setigera*). The second axis was mainly driven by the opposition between N_{off}-April and N_{off}-May (25% and 18% of total inertia, respectively) characterized by *P. pseudodelicatessima* (28%) and *D. fragilissimus* (32%), respectively. The third axis was mainly structured by the opposition between N_{off}-April and N_{off}-May exhibiting specific assemblages and stations showing characteristic spring/summer assemblages (Figure 4C, D). The factor analysis thus highlighted a strong heterogeneity of phytoplankton assemblages in late spring (April) evolving towards a common pattern in early summer (July).

Phytoplankton size spectra and composition

April showed the strongest heterogeneity between northern and southern waters as well as between inshore and offshore waters (Figures 4A, C & 5A). With the exception of N_{off}, small nanophytoplankton (<10 μm, *PgF* and cryptophyceans, Table 4) outnumbered phytoplankton taxa and represented 42 to 55% of total abundance. 20–100 μm microphytoplankters were the second dominant group (15–68%) comprising the potentially toxic diatom *P. pseudodelicatissima* in N_{off} (112.4 × 10^3 cell l^{-1}; 63% relative abundance) and *Melosira* sp., *Diploneis* sp. and *N. transitans* in the three other locations (0.2–12.7 × 10^3 cell l^{-1}). Larger diatoms (100–200 μm) were responsible for the spatial heterogeneity observed in southern waters. S_{in} was characterized by a typical shallow coastal assemblage dominated by *G. striata* and accompanied by *C. pelagica*, *R. amphiceros* and *N. longissima* (Table 4). In contrast, S_{off} had a more neritic pattern as *G. striata* was accompanied here by the large centric chain forming diatoms *D. brightwelli* and *O. sinensis* (100–200 μm; Table 4).

April to May transition was marked by a strong change in phytoplankton assemblages (Figure 4) characterized by a decrease in nanophytoplankton abundance (<6%) and an increase in the 20–100 μm (10–44%) and larger size fractions (100–200 μm and >200 μm; 15–57%; Figure 5B). *Gyrodinium striata* still dominated phytoplankton assemblages and was associated either to *D. fragilissimus* offshore (N_{off}) or *P. pseudodelicatissima* and *G. delicatula* inshore (N_{in}). Southern waters of the Bay of Somme (S_{in}) were characterized by the dominance of large diatoms (>200 μm; 57% of total phytoplankton), particularly *R. imbricata*. Intermediate (*L. danicus*) and large sized diatoms (*G. striata* and *O. sinensis*) identical to those observed in the north were also present (Table 4; Figure 4B, D).

Summer phytoplankton assemblages distribution and composition were relatively homogeneous (Figure 6) and dominated by large sized cells (100–200 μm and >200 μm), in particular *G. striata* (55–75%) and *R. imbricata* (17–19%; Table 4; Figure 5C). These two diatoms coexisted with intermediate sized diatoms (*G. delicatula* and *L. danicus*) and nanophytoplankton taxa such as cryptophyceans and small unidentified dinoflagellates. While this pattern of distribution was common to all locations, the 10–20 μm size fraction and particularly the small *Chaetoceros* sp. showed a markedly high contribution (16%) to the summer phytoplankton composition of Station S_{in} (Table 4; Figure 4B, D).

Phytoplankton diversity

Phytoplankton diversity (H') and evenness (J') ranged from 0.91 (S_{off}-July) to 1.82 (N_{in}-April) and from 0.38 (S_{off}-July) to 0.67 (N_{in}-April), respectively. With the exception of Station S_{in}, both indices followed a decreasing temporal pattern during the spring to summer transition (Table 5).
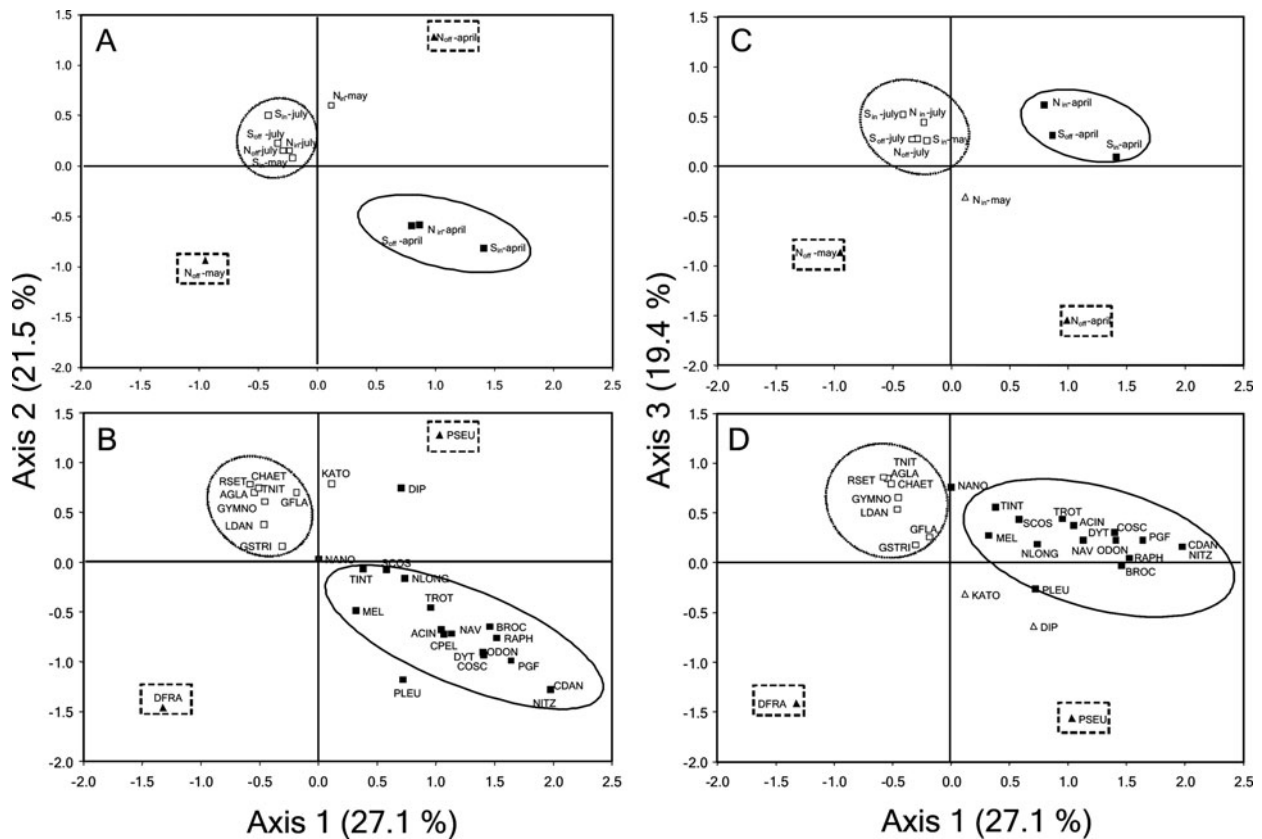
Fig. 4. Results of the factorial correspondence analysis conducted on phytoplankton taxa. Observations (stations) and variables (phytoplankton taxa; see Table 4 for details of the species codes) are presented separately. The plan on the first 3 axes described 68.1% of the total inertia. Projections of observations (A) and variables (B) in the two-dimensional plan defined by axes 1 and 2. Projections of observations (C) and variables (D) in the two-dimensional plan defined by axes 1 and 3. (■) Characteristic spring (April) and (□) summer (May/July) community. Specific taxa of N_{off}-April and N_{off}-May (▲).

Both temporal changes and spatial variability in the structure of phytoplankton assemblages clearly appeared on RFD diagrams (Figure 6). In April, RFDs exhibited distinct shape within each studied station highlighting the strong spatial heterogeneity of phytoplankton assemblages at the end of the *P. globosa* bloom (Figure 6). RFDs of northern coastal (N_{in}) and southern offshore (S_{off}) assemblages exhibited convex shapes over the first ranks. This indicated an even distribution of individuals among dominant species with high diversity index (1.51–1.82) and evenness (0.61–0.67) despite rather low species richness (12–15). In contrast, the RFDs in N_{off} and S_{in} respectively showed the dominance of *P. pseudodelicatissima* and *P. globosa*. This was related to lower diversity (1.30 to 1.78), lower evenness (0.48–0.57) and higher richness (15–23). From May to July, the structure of the phytoplankton assemblages evolved *via* intermediate distinct stages towards a similar RFD pattern, illustrating a shift in phytoplankton assemblage structure from four distinct spring structures to a common late spring–summer composition. In particular, the shape of the four RFDs illustrated the dominance of *G. striata* related to lower diversity and evenness in the entire area compared to April. In coastal waters (N_{in} and S_{in}), July RFDs were also characterized by a series of successive steps illustrating the presence of a more diversified diatom community (H': 1.54–1.56; S': 20–21) in inshore waters compared to offshore ones (H': 0.91–1.12; S':11–15).

Distances values (d) identified strong differences in the rank structure of phytoplankton assemblages between sampling sites throughout the survey (Table 6). In April, the highest distance was observed between N_{in} and S_{in} ($d = 6.67$), revealing distinct rank distribution among common species between northern and southern coastal assemblages. In contrast, the lowest d value was observed between N_{off} and S_{off} ($d = 4.20$), illustrating a more common pattern between offshore assemblages. In July, with the exception of the value calculated between N_{off} and S_{off} ($d = 4.12$) distances were relatively high between sampling sites (5.33–5.75) showing strong differences among common species distribution. The highest d values were observed between inshore and offshore assemblages on both studied zones, 5.74 in the Strait of Dover and 5.75 in the Bay of Somme (Table 6).

DISCUSSION

Phytoplankton succession during the wane of a *P. globosa* bloom

The Chl *a* concentrations ($<8\ \mu g\ l^{-1}$), *P. globosa* abundance (16.9×10^4 cell l^{-1}) and its contribution to phytoplankton biomass ($<25\%$) were low when compared to previous observation in the eastern English Channel in spring bloom conditions; i.e. Chl $a = 60\ \mu g\ l^{-1}$, abundance $= 10^6 - 10^7$ cell l^{-1} and 80% of total phytoplankton biomass (Breton *et al.*, 2000; Seuront *et al.*, 2006). The year 2003 was characterized by an early and short-term *P. globosa* bloom
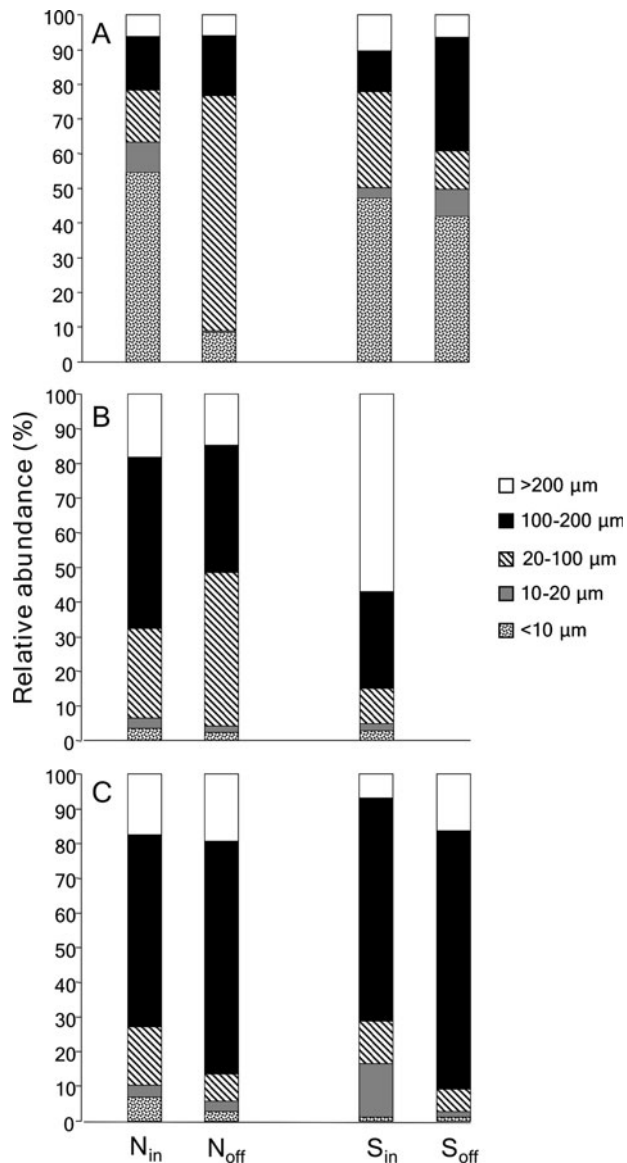
Fig. 5. Time course evolution of relative phytoplankton abundance (%) on the four sampling stations (N$_{in}$, N$_{off}$, S$_{in}$ and S$_{off}$) in April (A), May (B) and July (C), through five major size-categories: ≤10 µm, 10–20 µm, 20–100 µm, 100–200 µm, >200 µm. No data were available for S$_{off}$ in May.

which peaked in early March 2003 (Lamy et al., 2006; Muylaert et al., 2006) and disappeared rapidly by the end of April. This suggests, together with previous observations conducted in the Southern Bight of the North Sea (Lancelot, 1995; Rousseau et al., 2002; Tungaraza et al., 2003), that our April sampling occurred at the end of the P. globosa bloom. Microscopic observations also showed the development of hetero/mixotrophic ciliated protozoans within the samples, suggesting the existence of a potentially active microbial loop.

The main features of the wane of the P. globosa bloom observed during this survey are the occurrence of two consecutive diatom assemblages respectively dominated by: (i) small colonial species (<100 µm; namely Melosira sp., Diploneis sp. and N. transitans) co-occurring with P. globosa in April; and (ii) large fine-walled species (>200 µm; G. striata and R. imbricata) in May and July (Table 4; Figure 5). Similar patterns of diatom succession have been

previously reported at the seasonal scale in the eastern English Channel (Breton et al., 2000; Seuront et al., 2006) and the coastal waters of the North Sea (Gieskes & Kraay, 1975; Cadée & Hegeman, 1986; Rousseau et al., 2000, 2002; Tungaraza et al., 2003; Stelfox-Widdicombe et al., 2004; Muylaert et al., 2006). The key feature of these two consecutive diatom assemblages relies on their different nutrient conditions (Table 2) and the related potential nutrient limitation (Figure 3).

The assemblage of small diatoms co-occurring with P. globosa in April was potentially limited by nitrate. This is congruent with previous hydrological surveys conducted in the eastern English Channel showing nitrate depletion during the late phase of the P. globosa bloom (Brunet et al., 1992; Gentilhomme & Lizon, 1998). This may have favoured the development of small cells over larger forms in accordance with theoretical (Irwin et al., 2006) and field observations (Chisholm, 1992; Li, 2002). Resource limitation has been shown to alter size scaling metabolic rates, resulting in a decrease in the size scaling exponent (Finkel, 2001; Finkel et al., 2004). Several other factors may, however, have also contributed to the observed size structure of the diatom community in April, e.g. size dependent grazing (Armstrong, 2003), particles sinking and coagulation dynamics (Burd & Jackson, 2002; Stemman et al., 2004), size dependent physiological strategies such as surge uptake or storage capacities (Stolte et al., 1994; Stolte & Riegman, 1995).

The growth of the small chain-forming diatoms in April is also likely to lead to a potential silicic acid limitation through silicate depletion in May. This is consistent with the observed shift towards larger fine-walled diatoms (e.g. G. striata and R. imbricata), known to have lower silicate requirements (0.05 ≤ Si:C ≤ 0.10) than the small diatoms (0.17 ≤ Si:C ≤ 0.30) co-occurring with the P. globosa during spring in the North Sea (Rousseau et al., 2002). These genera appear to be particularly well adapted to low silicate concentrations as they have been reported to form large blooms in different coastal areas under silicate limitation (Sournia, et al., 1987; Del Amo et al., 1997a, b; Rousseau et al., 2002).

Finally, the increase in nutrient concentrations observed between May and July allowed the growth of the second diatom assemblage, leading to the relatively high phytoplankton biomass observed in coastal waters in July (Table 2). The increase in nutrient concentrations observed in July might be related to a combination of: (i) run-off inputs following rainfall events; (ii) high remineralization processes following the wane of the P. globosa bloom; (iii) sedimentary mineralization of silicate (Del-Amo et al., 1997b), phosphate (Auby et al., 1999) and nitrogen (Riou, 1999); or (iv) zooplankton excretion (Le Borgne, 1986).

From distinct spring structures to a common summer pattern

The eastern English Channel is characterized by two hydrological systems located in the Strait of Dover and the Bay of Somme, the former and the latter including hydrologically distinct inshore and offshore water masses (Table 2; Brylinski et al., 1991). Whilst these hydrological differences were clearly observed throughout the survey, phytoplankton assemblages only exhibited a strong spatial heterogeneity in April, and evolved towards a relative homogeneous structure in July.

Table 4. Code (used to identify species in factorial correspondence analysis), length (μm), presence (+)/absence (−), first (1)/secondary (2) dominant phytoplankton taxa identified from Lugol's iodine-preserved samples collected on the four sampling stations N_{in}, N_{off}, S_{in} and S_{off} during the survey. No data were available for S_{off} in May.

Taxa	Code	Length (μm)	N_{in} April	May	July	N_{off} April	May	July	S_{in} April	May	July	S_{off} April	May	July
Prymnesiophyceans														
PgF	PGF	5	2	+	−	+	+	+	1	+	+	1		+
Cryptophyceans														
Cryptophyta sp.	CRY	5	1	−	+	+	+	+	+	+	+	+		−
Diatoms														
Coscinodiscus sp	COSC	50	−	−	−	−	−	−	+	+	−	−		−
Skeletonema costatum	SCOS	7.5	+	+	−	−	−	−	+	−	+	−		−
Asterionellopsis glacialis	AGLA	60	−	−	+	−	−	−	−	−	+	−		−
Broeckmaniella brockmanni	BROC	15	−	+	−	−	−	−	+	−	−	−		−
Chaetoceros sp.	CHAET	20	−	+	−	−	+	+	+	−	2	−		−
Chaetoceros danicus	CDAN	20	−	−	−	−	−	−	+	−	−	−		−
Chaetoceros socialis	CSOC	12	−	+	+	−	−	−	−	−	−	−		−
Diploneis sp.	DIP	60	+	+	−	+	−	−	−	−	−	−		−
Ditylum brightwelli	DYT	150	−	−	+	−	−	−	+	−	−	−		−
Cerataulina pelagica	CPEL	40	−	−	−	−	−	+	+	+	−	+		+
Guinardia striata	GSRTI	140	+	1	1	2	2	1	2	2	1	2		1
Guinardia flaccida	GFLA	150	+	+	+	+	+	−	−	−	+	−		−
Guinardia delicatula	GDEL	30	−	+	+	+	−	−	+	−	+	−		−
Dactyliosolen fragilissimus	DFRA	65	−	−	−	−	1	+	−	−	−	−		−
Leptocylindrus danicus	LDAN	35	−	−	+	+	+	+	−	+	+	−		+
Thalassiosira rotula	TROT	20	−	−	−	−	−	−	+	−	+	−		−
Thalassionema nitzschioides	TNIT	7	−	−	−	−	−	−	−	−	+	−	−	−
Melosira sp.	MEL	20	+	+	+	−	+	+	+	+	−	+		+
Navicula transitans	NAV	45	+	+	+	−	+	−	+	+	+	−		−
Nitzschia longissima	NLONG	142	+	+	+	−	−	−	+	+	−	−		−
Nitzschia sp.	NITZ	40	−	−	−	−	−	−	+	−	−	−		−
Raphoneis amphiceros	RAPH	40	+	+	+	+	−	−	+	+	−	+		−
Ditctyocha sp.	DICT	10	−	−	+	−	−	−	−	−	−	−		−
Pleurosigma sp.	PLEU	225	+	−	+	−	+	−	+	+	−	−		−
Odontella sinensis	ODON	150	−	−	−	−	−	−	+	+	−	−		−
Rhizosolenia setigera	RSET	420	−	−	−	−	−	−	−	−	+	−		−
Rhizosolenia imbricata	RIMB	300	+	+	2	+	+	2	+	1	+	+		2
Pseudonitzschia pseudodelicatissima	PSEU	35	+	2	+	1	+	−	+	+	+	+		−
Dinoflagellates														
Protoperidinium sp.	PROTO	25	−	+	+	−	−	+	−	+	+	−		+
Katodinium sp.	KATO	25	−	−	−	+	−	+	−	−	+	+		+
Prorocentrum micans	PRORO	50	−	−	+	−	−	−	−	−	−	−	−	−
Torodinium sp.	TORO	15	−	+	−	+	−	+	+	+	+	+	+	+
Gymnodinium sp.	GYMNO	25	−	+	+	+	+	+	−	−	+	−		+

Table 4. Continued

Taxa	Code	Length (μm)	N_{in} April	May	July	N_{off} April	May	July	S_{in} April	May	July	S_{off} April	May	July
Gyrodinium sp.		65	−	−	−	−	−	−	−	+	−	−		−
Gyrodinium lachryma		160	+	+	−	−	+	+	+	+	−	−		−
Nanoflagellates	NANO	50	+	+	+	+	+	+	−	−	+	+		+
Ciliates														
Tintinnides	TINT	60	+	+	−	−	−	−	+	−	+	+		−
Aloricate ciliates	ACIL	33	+	+	+	+	+	+	+	+	+	+		+
Myrionecta rubra	MRUB	35	+	+	+	+	+	+	+	−	−	+		−
Acineta sp.	ACIN	50	+	−	−	−	−	−	+	+	+	−		−

Specific phytoplankton communities were identified in April in each of the four investigated water masses. This spatial heterogeneity led to a strong community gradient in terms of abundance, composition and distribution (Tables 3–4; Figures 4–6). In particular, *P. globosa* and flagellates dominated the community in S_{in}, but occurred in very low abundance in N_{off}, while co-dominance with either cryptophyceans or the diatom *G. striata* was observed in N_{in} and S_{off}, respectively. The control of *P. globosa* blooms magnitude by nitrate remaining after the early diatom bloom (Lancelot, 1995; Lancelot *et al.*, 1998) and the relatively high nitrate concentrations recorded when *P. globosa* dominated the phytoplankton pool (0.54 μM; Table 2) suggest that differential nitrate concentrations could have driven the observed spatial patterns. Alternatively, limited nutrient supplies as well as strong turbulent conditions prevailing in the Strait of Dover (Seuront, 2005; Seuront & Schmitt, 2005) may have supported cryptophycean growth, which are typical 'stress-tolerant' species (Margalef, 1958) and known to occur after disturbances (Barbiero *et al.*, 1999). In addition, high distances between rank distributions among common species revealed that this spatial heterogeneity was not only restricted to dominant species. This spatial heterogeneity illustrates the concept of life forms adaptation to specific pelagic habitats (i.e. ecological niches) defined along gradients of turbulence intensity and nutrient concentrations (Margalef, 1978; Cullen *et al.*, 2002). Within a given location, phytoplankton assemblages are thus dominated and composed of species that are best adapted to the local environmental forcing.

In contrast, early summer was characterized by the dominance of 'generalist' taxa (*sensu* Margalef, 1978), *G. striata* and *R. imbricata*. These taxa are intrinsically not constrained to defined niches and therefore dominated phytoplankton assemblages in the whole area. The high distances observed between rank organizations nevertheless suggest a strong heterogeneity among small (<100 μm) secondary species distribution, particularly between inshore and offshore waters. The co-existence of large and small diatoms within a given phytoplankton assemblage is not rare (Dupuy *et al.*, 2000; Vincent *et al.*, 2002) and often results from punctual nutrient inputs following climatic events (e.g. stormy events; Vincent *et al.*, 2002) as observed in May and July. Local hydrological properties prevailing in each area may thus have led to the establishment of specific small secondary species as illustrated by the small *Chaetoceros* sp. and dinoflagellates restricted to the warmer waters of the Bay of Somme in July.

From mature/senescent communities to a pioneer community

The shape of the RFDs, and more specifically their changes in space and/or time, reveals the degree of organization and complexity of the ecosystem and thus is related to its degree of maturity. At the end of the *P. globosa* bloom (April), the shape of the RFDs obtained in N_{in} and S_{off} indicated an even distribution of individuals among dominant species which is characteristic of mature assemblages (Frontier, 1985). The RFDs obtained in S_{in} and N_{off} exhibited a more rectilinear shape, suggesting a senescent stage of the community. This is expected at the end of an ecological succession, when one species (here *P. globosa* in S_{in}/*P. pseudodelicatessima* in N_{off}) is in exceptionally favourable conditions and
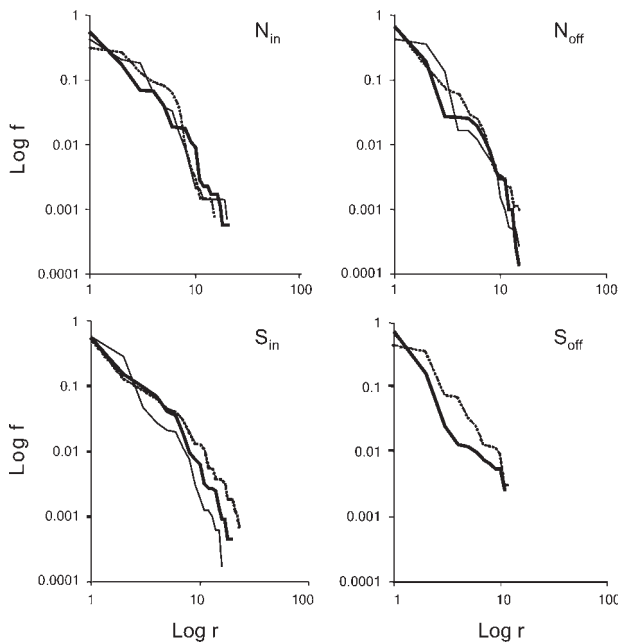
Fig. 6. Rank–frequency diagrams of phytoplankton species for the four sampling stations (N_{in}, N_{off}, S_{in} and S_{off}) in April (dotted line), May (continuous line) and July (bold line). No data were available for S_{off} in May.

escapes the demographic control exerted by others (Frontier, 1985). The April mature/senescent communities were followed by the establishment of a pioneer community characterized by the generalist taxa *G. striata* and *R. imbricata*. This is illustrated by a decrease in diversity and evenness as well as the vertical shape of RFDs observed on the entire area in July. This kind of community typically occurs after disturbances or fast changes of the environment (Frontier, 1985).

The *P. globosa* bloom may have induced strong changes in the pelagic environment leading to a new colonization, after the loss of some of the previous sets of species (Frontier, 1985). After a transition stage (May), a few species (*G. striata* and *R. imbricata*) may have imposed their dominance through their highest tolerance to the more drastic conditions (i.e. silicate limitation) prevailing on the entire studied area after the collapse of the bloom. Although nutrients concentration is often considered as a key factor controlling phytoplankton succession and species success (Rees *et al.*, 1999),

Table 5. Species richness (S), diversity index (H′) and evenness (J′) of phytoplankton community, on the four sampling stations N_{in}, N_{off}, S_{in} and S_{off} during the survey. No data were available for S_{off} in May.

Station	Period	S	H′	J′
N_{in}	April	15	1.82	0.67
	May	20	1.65	0.55
	July	21	1.54	0.50
N_{off}	April	15	1.30	0.48
	May	15	1.32	0.49
	July	15	1.12	0.41
S_{in}	April	23	1.78	0.57
	May	16	1.23	0.44
	July	20	1.56	0.52
S_{off}	April	12	1.51	0.61
	May	–	–	
	July	11	0.91	0.38

Table 6. Distance (d) between rank distributions of phytoplankton species identified on 2 distinct sampling sites during the survey. d(N_{in}–N_{off}) and d(S_{in}–S_{off}): distances between inshore and offshore waters within the same studied site; d(N_{in}–S_{in}) and d(N_{off}–S_{off}): distances between inshore/offshore waters of both studied sites. No data were available for S_{off} in May.

	April	May	July
d (N_{in}–N_{off})	4.59	3.51	5.74
d (S_{in}–S_{off})	6.15	–	5.75
d (N_{in}–S_{in})	6.67	3.45	5.33
d (N_{off}–S_{off})	4.20	–	4.12

nutritive status alone is not a totally satisfactory explanation for the observed evolution of phytoplankton assemblages. During our survey, micro- and mesozooplankton consumers may have also played a pivotal role in controlling phytoplankton diversity through grazing and nutrient regeneration. Various critical processes shaping the structure and function of the microbial loop developed in April (e.g. excretion and bacterial degradation) may have led to massive and local inorganic nitrogen release (particularly NH_4^+). The nutrient enrichment related to high grazing activity within the microbial loop (Stelfox-Widdicombe *et al.*, 2004) and lagged time response of metazoan consumers (Malone, 1992), may also have enhanced large-diatom production in early summer as previously shown by Duarte *et al.* (2000). Finally, the accumulation of dissolved polymeric materials during the collapse of the *P. globosa* bloom, believed to induce foam formation in the surf zone (Lancelot, 1987; Rousseau, 2000; Peperzak, 2002), may have influenced phytoplankton diversity. In the coastal waters of the Bay of Somme (S_{in}) where highest densities of *P. globosa* were recorded in April, species richness strongly decreased between April and May (from 23 to 16). While highly speculative, it is suggested that this may be related to the loss of biomass entrained within the foam following the release of dissolved polymeric materials by senescent colonies (Seuront *et al.*, 2006). The decrease in competition following this non-negligible loss of phytoplankton population, may then have allowed remaining species such as *R. imbricata* and *G. striata* to grow quickly and thus colonize this new environment.

Concluding remarks

Previous studies have investigated the seasonal succession of phytoplankton communities in the eastern English Channel (Breton *et al.*, 2000; Seuront *et al.*, 2006) and the North Sea (Rousseau *et al.*, 2002). We specifically focused here on the collapse of the *P. globosa* bloom and followed the evolution of phytoplankton assemblages in four distinct hydrological sub-systems. Specific phytoplankton assemblages identified in distinct water masses during the late phase of the bloom (April), have evolved from a mature/senescent community towards a relatively homogeneous summer structure. This suggests the establishment of a pioneer community on the entire studied area as a result of complex interactions between different hydrological and biological processes. In particular, low silicic acid is suggested to be an essential factor favouring the establishment of a summer pioneer community dominated by large fine-walled diatoms (*G. striata* and *R. imbricata*). Although the same evolution was observed

over the entire study area, suggesting similar dynamics in distinct hydrological sub-systems, the magnitude of the observed patterns is intrinsically related to the hydrological properties prevailing in each sub-system.

Finally, it is stressed that additional field and laboratory experiments are still needed: (i) to assess the role played by micro- and mesozooplankton consumers; and (ii) to confirm the potential effect of foam formation following the wane of a *P. globosa* bloom on the seasonal evolution of phytoplankton assemblages in the eastern English Channel. As the pathways and efficiencies of energy transfer from primary producers to consumers and ultimately the production of higher trophic levels are determined by phytoplankton composition (Cloern & Dufford, 2005), the establishment of a poorly diversified pioneer community following the wane of a *P. globosa* bloom may have strong consequences on food web dynamics and the carbon cycle in coastal ecosystems. The genus *Phaeocystis* may thus play a key role in the ocean–atmosphere transfers especially considering this occurrence in very contrasted marine systems from the northern (Lancelot, 1998) to the southern hemisphere (LeRoi & Hallegraeff, 2006).

REFERENCES

Armstrong R.A. (2003) A hybrid spectral representation of phytoplankton growth and zooplankton response: the 'control rod' model of plankton interaction. *Deep-Sea Research II* 50, 2895–2916.

Auby I., Trut G., D'Amico F. and Beliaeff B. (1999) *Réseau hydrologique du Bassin d'Arcachon. Synthèse des résultats 1988–1997.* Rapport interne IFREMER/DEL, Arcachon, France.

Azam F., Fenchel T., Field J.G., Gray J.S., Meyer-Reil L.A. and Thingstad F. (1983) The ecological role of water-column microbes in the sea. *Marine Ecology Progress Series* 10, 257–263.

Badylak S. and Phlips E.J. (2004) Spatial and temporal patterns of phytoplankton composition in a subtropical coastal lagoon, the Indian River Lagoon, Florida, USA. *Journal of Plankton Research* 26, 1229–1247.

Barbiero R.P., James W.F. and Barko J.W. (1999) The effects of disturbance events on phytoplankton community structure in a small temperate reservoir. *Freshwater Biology* 42, 503–512.

Bendschneider K. and Robinson R.J. (1952) A new spectrophotometric method for determination of nitrite in the sea water. *Journal of Marine Research* 2, 87–96.

Bode A., Alvarez-Ossorio M.T., Gonzalez N., Lorenzo J., Rodriguez C., Varela M. and Varela M.M. (2005) Seasonal variability of plankton blooms in the Ria de Ferrol (NW Spain): II. Plankton abundance, composition and biomass. *Estuarine, Coastal and Shelf Science* 63, 285–300.

Breton E., Brunet C., Sautour B. and Brylinski J.M. (2000) Annual variations of phytoplankton biomass in the Eastern English Channel: comparison by pigment signatures and microscopic counts. *Journal of Plankton Research* 22, 1423–1440.

Brunet C., Brylinski J.M. and Frontier S. (1992) Productivity, photosynthetic pigments and hydrology in the coastal front of the Eastern English Channel. *Journal of Plankton Research* 14, 1541–1552.

Brunet C., Brylinski J.M. and Lemoine Y. (1993) *In situ* variations of the xanthophylls diatoxanthin and diadinoxanthin: photoadaptation and relationships with a hydrodynamical system in the Eastern English Channel. *Marine Ecology Progress Series* 102, 69–77.

Brunet C., Davoult D. and Casotti R. (1996) Physiological reactions to a change in light regime in cultured *Skeletonema costatum* (Bacilloriophyta): implications for estimation of phytoplankton biomass. *Hydrobiologia* 333, 87–94.

Brylinski J.M., Dupont J. and Bentley D. (1984) Conditions hydrologiques au large du Cap Gris-Nez (France): premiers résultats. *Oceanologica Acta* 7, 315–322.

Brylinski J.M. and Lagadeuc Y. (1990) L'interface eaux côtières/eaux du large dans le Pas de Calais (côte française): une zone frontale. *Comptes Rendus de l'Académie des Sciences* 311 série II, 535–540.

Brylinski J.M., Lagadeuc Y., Gentilhomme V., Dupont J.P., Lafite R., Dupeuple P.A., Huault M.F., Auger Y., Puskaric E., Wartel M. and Cabioch L. (1991) Le fleuve côtier: un phénomène hydrologique important en Manche Orientale. Exemple du Pas de Calais. *Oceanologica Acta* 11, 197–203.

Brylinski J.M., Brunet C., Bentley D., Thoumelin G. and Hilde D. (1996) Hydrography and phytoplankton biomass in the Eastern English Channel in spring 1992. *Estuarine, Coastal and Shelf Science* 43, 507–519.

Brzezinski M.A. (1985) The Si:N:P ratio of marine diatoms: interspecific variability and the effect of some environmental variables. *Journal of Phycology* 21, 347–357.

Burd A.B. and Jackson G.A. (2002) Modelling steady-state particle size spectra. *Environmental Sciences and Technology* 36, 323–327.

Cadée G.C. and Hegeman J. (1986) Seasonal and annual variations in *Phaeocystis pouchetii* (Haptophyceae) in the westernmost inlet of the Wadden Sea during the 1973 to 1985 period. *Netherland Journal of Sea Research* 20, 29–36.

Chang A.T. (1980) Comparative physiological study of marine diatoms and dinoflagellates in relation to irradiance and cell size. II. Relationship between photosynthesis, growth and carbon/chlorophyll *a* ratio. *Journal of Phycology* 16, 428–432.

Chang F.H., Zeldis J., Gall M. and Hall J. (2003) Seasonal and spatial variation of phytoplankton assemblages, biomass and cell size from spring to summer across the north-eastern New Zealand continental shelf. *Journal of Plankton Research* 25, 737–758.

Chisholm S.W. (1992) Phytoplankton size. In Falkowski P.G. and Woodhead A.D. (eds) *Primary productivity and biogeochemical cycles in the sea.* New York: Plenum Press, pp. 213–237.

Cloern J.E. and Dufford R. (2005) Phytoplankton community ecology: principles applied in San Francisco Bay. *Marine Ecology Progress Series* 285, 11–28.

Cullen J.J., Franks P.S., Karl D.M. and Longhurst A. (2002) Physical influences on marine ecosystem dynamics. In Robinson A.R., McCarthy J.J. and Rothschild B.J. (eds) *The sea*, Vol. 12. New York: John Wiley & Sons, pp. 297–336.

Del Amo Y., Le Pape O., Tréguer P., Quéguiner P., Ménesguen A. and Aminot A. (1997a) Impacts of high-nitrate freshwater inputs on macrotidal ecosystems. I. Seasonal evolution of nutrient limitation for the diatom-dominated phytoplankton in the Bay of Brest (France). *Marine Ecology Progress Series* 161, 213–224.

Del Amo Y., Quéguiner B., Tréguer P., Breton H. and Lampert L. (1997b) Impacts of high-nitrate freshwater inputs on macrotidal ecosystems. II. Specific role of the silicic acid pump in the year-round dominance of diatoms in the Bay of Brest (France). *Marine Ecology Progress Series* 161, 225–237.

Duarte C.M., Agusti S. and Kalff J. (2000) Particulate light absorption and the prediction of phytoplankton biomass and planktonic metabolism in Northeastern Spanish aquatic ecosystems. *Canadian Journal of Fisheries and Aquatic Sciences* 57, 25–33.

Dupont J.P., Lafite R., Huault M.F., Lamboy M., Brylinski J.M. and Guéguéniat P. (1991) La dynamique des masses d'eau et matières en suspension en Manche Orientale. *Oceanologica Acta* 11, 177–186.

Dupuy C., Vaquer A., Lam-Hoai T., Rougier C., Mazouni N., Lautier J., Collos Y. and Le Gall S. (2000) Feeding rate of the oyster *Crassostrea gigas* in a natural plankton community on the Mediterranean Thau Lagoon. *Marine Ecology Progress Series* 205, 171–184.

Estrada M., Henriksen P., Gasol J.M. Casamayor E.O. and Pedros-Alio C. (2004) Diversity of planktonic photoautotrophic microorganisms along a salinity gradient as depicted by mircoscopy, flow cytometry, pigment analysis and DNA-based methods. *FEMS Microbiology and Ecology* 49, 281–293.

Finkel Z.V. (2001) Light absorption and size scaling of light-limited metabolism in marine diatoms. *Limnology and Oceanography* 46, 1, 86–94.

Finkel Z.V., Irwin A.J. and Schofield O. (2004) Resource limitation alter the 3/4 size scaling of metabolic rates in phytoplankton. *Marine Ecology Progress Series* 273, 269–279.

Frontier S. (1976) Utilisation des diagrammes rangs-fréquences dans l'analyse des écosystèmes. *Journal de la Recherche Océanographique* 1, 35–48.

Frontier S. (1985) Diversity and structure in aquatic ecosystems. *Oceanography and Marine Biology: an Annual Review* 23, 253–312.

Gentilhomme V. and Lizon F. (1998) Seasonal cycle of nitrogen and phytoplankton biomass in a well-mixed coastal system (Eastern English Channel). *Hydrobiologia* 361, 191–199.

Gieskes W.W.C. and Kraay G.W. (1975) The phytoplankton spring bloom in Dutch coastal waters of the North Sea. *Netherland Journal of Sea Research* 9, 166–196.

Grabemann I. and Krause G. (2001) On different time scales of suspended matter dynamics in the Weser estuary. *Estuaries* 24, 688–698.

Hamm C.E. (2000) Architecture, ecology and biogeochemistry of *Phaeocystis* colonies. *Journal of Sea Research* 43, 307–315.

Harris G.P. (1978) Photosynthesis, productivity and growth; the physiological ecology of phytoplankton. *Ergebneim Limnology* 10, 1–171.

Hasle G.R., Syversten E.E., Steidinger K.A., Throndsen J. and Heimdal B.R. (1997) *Identifying marine phytoplankton*. St Petersburg, Russia and Florida, USA: CRT.

Hillebrand H., Dürselen C.D., Kirschtel D., Pollingher D. and Zohary T. (1999) Biovolume calculation for pelagic and benthic microalgae. *Journal of Phycology* 35, 403–424.

Huault M.F., Lafite R. and Dupont J.P. (1994) Diatoms as particulate tracers in the water column in the Eastern English Channel. *Netherland Journal of Sea Research* 33, 47–56.

Irwin A.J., Finkel Z.V., Schofield O.M.E. and Falkowski P.G. (2006) Scaling-up from nutrient physiology to the size structure of phytoplankton communities. *Journal of Plankton Research*, 28, 5, 459–471.

Koroleff F. (1969) Direct determination of ammonia in natural waters as indophenol blue. *International Council for the Exploration of the Sea* 9, 1–6.

Lagadeuc Y., Brylinski J.M. and Aelbrecht D. (1997) Temporal variability of the vertical stratification of a front in a tidal region of freshwater influence (ROFI) system. *Journal of Marine Research* 12, 147–155.

Lamy D., Artigas L.F., Jauzein C., Lizon F. and Cornille V. (2006) Coastal bacterial viability and production in the eastern English Channel: a case study during a *Phaeocystis globosa* bloom. *Journal of Sea Research* 56, 227–238.

Lancelot C. (1987) *Phaeocystis* blooms and nutrient enrichment in the continental coastal zones of the North Sea. *Ambiology* 16, 38–46.

Lancelot C. (1995) The mucilage phenomenon in the continental coastal waters of the North Sea. *The Science of the Total Environment* 165, 83–102.

Lancelot C. (1998) Autoecology in the marine haptophyte *Phaeocystis* sp. In Anderson D.M., Cembella A.D. and Hallegraeff G. (eds) *Physiological ecology of harmful algal blooms*. Berlin, Heidelberg: Springer-Verlag, pp. 209–224.

Lancelot C., Wassemann P. and Barth H. (1994) Ecology of *Phaeocystis*-dominated ecosystems. *Journal of Marine Systems* 5, 1–4.

Le Borgne R. (1986) The release of soluble end products of metabolism. In Corner E.D. and O'Hara S.C.M. (eds) *The biological chemistry of marine copepods*. New York: Clarendon Press, pp. 109–164.

Legendre P. and Legendre L. (1998) *Numerical ecology*. 2nd English edition. Amsterdam: Elsevier Science.

LeRoi J.M. and Hallegraeff G.M. (2006) Scale-bearing nanoflagellates from Southern Tasmania coastal waters, Australia. II. Species of Chrysophyceae (Chrysophyta), Prymnesiophyceae (Haptophyta, excluding Chrysochromulina) and Prasinophyceae (Chlorophyta). *Botanica Marina* 49, 213–235.

Li W.K.W. (2002) Macroecological patterns of phytoplankton in the northwestern North Atlantic Ocean. *Nature* 419, 154–157.

Malone T.C. (1992) Effects of water column processes on dissolved oxygen, nutrients, phytoplankton and zooplankton. In Smith D.E., Leffler M. and Mackiernan G. (eds) *Oxygen dynamics in the Chesapeake Bay. A synthesis of recent research*. College Park, MD: Maryland Sea Grant, pp. 61–112.

Margalef R. (1958) Temporal succession and spatial heterogeneity in plankton. In Buzzati-Traverso A.A. (ed.) *Perspectives in marine biology*. Berkeley: University of California Press, pp. 323–349.

Margalef R. (1978) Life forms of phytoplankton as survival alternatives in an unstable environment. *Oceanologica Acta* 1, 493–509.

Menden-Deuer S.E., Lessard J. and Satterberg J. (2001) Effect of preservation on dinoflagellates and diatom cell volume and consequences for carbon biomass predictions. *Marine Ecology Progress Series* 222, 41–50.

Menden-Deuer S.E. and Lessard E.J. (2000) Carbon to volume relationships for dinoflagellates, diatoms, and other protist plankton. *Limnology and Oceanography* 45, 569–579.

Mullin J.B. and Riley J.P. (1955) The colorimetric determination of silicate with special reference to sea and natural waters. *Analytica Chimica Acta* 12, 162–176.

Murphy J. and Riley J.P. (1962) A modified single solution method for determination of phosphate in natural waters. *Analytica Chimica Acta* 27, 31–36.

Muylaert K., Gonzales R., Franck M., Lionard M., Van der Zee C., Cattrijsse A., Sabbe K., Chou L. and Vyverman W. (2006) Spatial variation in phytoplankton dynamics in the Belgian coastal zone of the North Sea studied by microscopy, HPLC-CHEMTAX and under-way fluorescence recordings. *Journal of Sea Research* 55, 253–265.

Paulmier G. (1997) *Atlas des Diatomophycées des côtes françaises et des aires océaniques adjacentes.* IFREMER–DRV–RH–RST, 94. 14, 187 pp.

Peperzak L. (2002) *The wax and the wane of* Phaeocystis globosa *blooms.* PhD thesis. University Rijksuniversiteit Groningen, The Netherlands.

Pielou E.C. (1966) Species-diversity and pattern-diversity in the study of ecological succession. *Journal of Theoretical Biology* 10, 370–383.

Pingree R.D. and Griffiths D. (1980) Currents driven by a steady uniform wind stress on the shelf seas around the British Isles. *Oceanologica Acta* 3, 227–236.

Redfield A.C., Ketchum B.H. and Richards F.A. (1963) The influence of organisms on composition of seawater. *The Sea* 2, 26–77.

Rees A.P., Joint I. and Donald K.M. (1999) Early spring bloom phytoplankton–nutrient dynamics at the Celtic Sea Shelf Edge. *Deep-Sea Research II* 46, 483–510.

Riou S.A. (1999) *Cycle de l'azote à l'interface eau–sédiment dans le Bassin d'Arcachon: rôle des bactéries dans les processus de pertes en azote (nitrification–dénitrification).* PhD thesis. Université de Bordeaux I, France.

Rousseau V. (2000) *Dynamics of* Phaeocystis *and diatoms blooms in the eutrophicated coastal waters of the Southern Bight of the North Sea.* PhD thesis. Université Libre de Bruxelles, Belgium.

Rousseau V., Becquevort S., Parent J.Y., Gasparini S., Daro N., Tackx M. and Lancelot C. (2000) Trophic efficiency of the planktonic food web in a coastal ecosystem dominated by *Phaeocystis* colonies. *Journal of Sea Research* 43, 357–372.

Rousseau V., Leynaert A., Daoud N. and Lancelot C. (2002) Diatom succession, silicification and availability in Belgian coastal waters (southern North Sea). *Marine Ecology Progress Series* 236, 61–73.

Rousseau V., Vaulot D., Casotti R., Cariou V., Lenz J., Gunkel J. and Baumann M.E.M. (1994) The life cycle of *Phaeocystis* (Prymnesiophyceae): evidence and hypotheses. *Journal of Marine Systems* 5, 23–39.

Salomon J.C. and Breton M. (1991) An atlas of long-term currents in the Channel. *Oceanologica Acta* 16, 449–455.

Schapira M. (2005) *Space and time dynamic of* Phaeocystis globosa *in the eastern English channel: impact of turbulence and sporadic nutrients inputs.* PhD thesis. Université des Sciences et Techniques de Lille, France.

Seuront L. (2005) Hydrodynamical and tidal controls of small-scale phytoplankton patchiness. *Marine Ecology Progress Series* 302, 93–101.

Seuront L. and Schmitt F.G. (2005) Multiscaling statistical procedures for the exploration of biophysical couplings in intermittent turbulence. Part II. Applications. *Deep-Sea Research II* 52, 1325–1343.

Seuront L., Vincent D. and Mitchell J.G. (2006) Biologically-induced modification of seawater viscosity in the Eastern English Channel during a *Phaeocystis globosa* spring bloom. *Journal of Marine Systems* 61, 118–133.

Seymour J.R., Mitchell J.R. and Seuront L. (2004) Microscale heterogeneity in the activity of coastal bacterioplankton communities. *Aquatic Microbiology and Ecology* 35, 1–16.

Shannon C.E. and Weaver W. (1963) *The mathematical concept of communication.* Urbana: University of Illinois Press.

Sin Y., Wetzel R.L. and Anderson I.C. (2000) Seasonal variations of size-fractionated phytoplankton along the salinity gradient in the York River estuary, Virginia (USA). *Journal of Plankton Research* 22, 10, 1945–1960.

Sournia A., Birrien J.L., Douvillé J.L., Klein B. and Viollier M. (1987) A daily study of diatom spring bloom at Roscoff (France) in 1985. I. The spring bloom within the annual cycle. *Estuarine, Coastal and Shelf Science* 25, 355–367.

Stelfox-Widdicombe C.E., Archer S.D., Burkill P.H. and Stefels J. (2004) Microzooplankton grazing in *Phaeocystis* and diatom-dominated waters in the southern North Sea in spring. *Journal of Sea Research* 51, 37–51.

Stemmann L., Jackson G.A. and Ianson D. (2004) A vertical model of particles size distributions and fluxes in the midwater columns that includes biological and physical processes. I. Model formulation. *Deep-Sea Research I* 51, 865–884.

Stolte W., McCollin T. Noordeloos A.M.M. and Riegman R. (1994) Effect of nitrogen source on the size distribution within marine phytoplankton populations. *Journal of Experimental Marine Biology and Ecology* 184, 83–97.

Stolte W. and Riegman R. (1995) Effect of phytoplankton cell size on transient-state nitrate and ammonium uptake kinetics. *Microbiology* 141, 1221–1229.

Sun J. and Liu D. (2003) Geometric models for calculating cell biovolume and surface area for phytoplankton. *Journal of Plankton Research* 25, 1331–1346.

Tadonléké R.D. and Sime-Ngando T. (2000) Rates of growth and microbial grazing mortality of phytoplankton in a recent artificial lake. *Aquatic Microbial Ecology* 22, 301–313.

Tungaraza C., Rousseau V., Brion N., Lancelot C., Gichuki J., Baeyens W. and Goeyens L. (2003) Contrasting nitrogen up-take by diatom and *Phaeocystis*-dominated phytoplankton assemblages in the North Sea. *Journal of Experimental Marine Biology and Ecology* 292, 19–41.

Utermöhl H. (1958) Toward the improvement of the quantitative phytoplankton method. *Mitteilungen International Verieningung für Limnologie* 9, 1–39.

Van Rijssel M., Hamm C.E. and Gieskes W.W.C. (1997) *Phaeocystis globosa* (Prymnesiophyceae) colonies: hollow structures built with small amounts of polysaccharides. *European Journal of Phycology* 32, 185–192.

Venrick E.L. (1978) How many cells to count? In Sournia A. (ed.) *Phytoplankton manual.* Paris: UNESCO Press, pp. 167–180.

Vincent D., Luczak C. and Sautour B. (2002) Effects of a brief climatic event on zooplankton community structure and distribution in Arcachon Bay. *Journal of the Marine Biological Association of the United Kingdom* 82, 21–30.

Wolfstein K., Colijn F. and Doerffer R. (2000) Seasonal dynamics of microphytobenthos biomass and photosynthetics in the northern German Wadden sea, obtained by photosynthetic light dispersion system. *Estuarine, Coastal and Shelf Science* 51, 651–662.

Woods E.D., Armstrong F.A.J. and Richards F.A. (1967) Determination of nitrate in the sea water by cadmium–copper reduction to nitrite. *Journal of the Marine Biological Association of the United Kingdom* 47, 23–31.

and

Zar J.H. (1996) *Biostatistical analysis.* Upper Saddle River, New Jersey: Prentice-Hall International.

Correspondence should be addressed to:
Mathilde Schapira
School of Biological Sciences, Flinders University
GPO Box 2100, Adelaide SA 5001, Australia
email: mathilde.schapira@flinders.edu.au